Coordination Chemistry Reviews
198 (2000) 157–169

www.elsevier.com/locate/ccr

Novel layered structures constructed from iron–chloranilate compounds

M.K. Kabir [a], N. Miyazaki [a], S. Kawata [a,*], K. Adachi [a], H. Kumagai [b], K. Inoue [b], S. Kitagawa [c], K. Iijima [a], M. Katada [d]

[a] *Department of Chemistry, Faculty of Science, Shizuoka University, 836 Oya, Shizuoka 422-8529, Japan*
[b] *Institute for Molecular Science, Myoudaiji, Okazaki, Aichi 444-8585, Japan*
[c] *Department of Synthetic Chemistry and Biological Chemistry, Graduate School of Engineering, Kyoto University, Yoshida, Sakyo-ku, Kyoto 606-8501, Japan*
[d] *Department of Chemistry, Tokyo Metropolitan University, Minami Ohsawa, Hachiouji, Tokyo 192-0397, Japan*

Received 18 June 1999; accepted 14 December 1999

Contents

* Corresponding author. Tel./fax: +81-54-238-4757.
E-mail address: scskawa@ipc.shizuoka.ac.jp (S. Kawata)

PII: S0010-8545(00)00232-0

Abstract

Novel hydrogen bond-supported intercalation compounds, $\{(G)_m[Fe(CA)_2(H_2O)_2]\}_n$ (CA^{2-} = chloranilate, G = guest molecules) have been synthesized and characterized. The compound $\{(Hpy)[Fe(CA)_2(H_2O)_2](H_2O)\}_n$ (py = pyridine) (**1**) crystallizes in the triclinic, space group $P\bar{1}$ (#2), with $a = 9.537(5)$, $b = 13.563(6)$, $c = 9.231(4)$ Å, $\alpha = 107.18(4)$, $\beta = 102.33(4)$, $\gamma = 102.12(4)°$, $V = 1065.9(10)$ Å^3, and $Z = 2$. Compound $\{(H_2bipy)[Fe(CA)_2(H_2O)_2]_2(H_2O)_2\}_n$ (bipy = 4,4′-bipyridine) (**2**) crystallizes in the triclinic, space group $P\bar{1}$ (#2), with $a = 9.101(1)$, $b = 10.379(1)$, $c = 12.802(2)$ Å, $\alpha = 79.45(1)$, $\beta = 82.67(1)$, $\gamma = 66.32(1)°$, $V = 1086.8(3)$ Å^3, and $Z = 1$. The structure of **1** consists of mononuclear $[Fe(CA)_2(H_2O)_2]^-$ anions, Hpy^+ cations and uncoordinated water molecules. Four oxygen atoms of two CA^{2-} anions and two oxygen atoms from two water molecules are coordinated to the iron ion making anionic building blocks of the host layer. The compound of **2** contains the similar monomeric building blocks, H_2bipy^{2+} cations and uncoordinated water molecules. In both the compounds the coordination geometry of the building blocks are distorted octahedron, where two water molecules sit on the *trans* position in **1** and on the *cis* position in **2**. In compound **1** the $[Fe(CA)_2(H_2O)_2]^-$ anions make a two-dimensional (2-D) layer supported by hydrogen bonds. Hpy^+ ions are included in between the layers of **1** supported by hydrogen-bonding and electrostatic interaction with the host layers. In compound **2** the coordinated chloranilate rings of $[Fe(CA)_2(H_2O)_2]^-$ anions are stacked upon each other and make a layer with the help of hydrogen bonds. H_2bipy^{2+} cations are included in between the layers supported by hydrogen bonding, electrostatic and stacking interaction with coordinated CA^{2-} ions. The ^{57}Fe Mössbauer spectra of the compounds show that the oxidation state of iron is 3 with IS = 0.41 (**1**) and 0.39 mm s^{-1} (**2**); QS = 0.83 (**1**) and 1.29 mm s^{-1} (**2**) at 296 K, respectively. Compound **2** shows weak antiferromagnetic interaction over the crystal ($\theta = -2.3$ K).

Keywords: Inclusion compounds; Polyoxo-carbons; Metal complex assemblies

1. Introduction

The synthesis of transition metal complex-based two-dimensional (2-D) compounds is an important step in developing not only a new conductive and magnetic phase [1–12], but also an intercalation system for ion or molecule exchange, adsorption and catalytic properties [13]. Self-assembled infinite metal complexes with specific network topologies attract great attention due to their potential properties as functional solid materials as well as fascinating molecular structures [14–33]. The construction of suitable building block is a pioneering approach in the field of supramolecular chemistry. Intermolecular interactions that have been used to produce such suprastructures include coordination bonding [34–39], hydrogen bonding [13,40,41], and van der Waals forces such as stacking interactions [13]. The hydrogen bonding interaction especially plays an important role for the construction of higher dimensional metal complex assemblies [41–44], which provide novel dynamic and thermochromic properties of the crystals [45–49]. This interaction is

specific and directional and has little dependence on the properties of metal ions, readily providing extended arrays [50–53]. Thus, one of the best strategies for the rational synthesis of crystalline metal assembled complexes is to utilize the hydrogen bonding capability of coordinated ligands in addition to their coordination capability [13]. Polyoxo-carbon compounds are well known to be double bidentate ligands, and are good candidates to provide transition metal complex assemblies [54]. Chloranilic acid is one of that family, affording one-dimensional (1-D) chains of various metal ions [55–59,64–66]. Interestingly, in most of all coordination polymers of oxocarbons, the hydrogen-bonding interaction plays an important role to construct extended arrays. Very recently, taking advantage of the strong hydrogen-bonding ability of the pyridine–hydroxyl group and the oxocarbon–hydroxyl group, we have succeeded in synthesizing the novel intercalation compounds containing straight 1-D chains, $[M(CA)(H_2O)_2]_m$ ($M = Mn^{2+}$, Fe^{2+}, Co^{2+}, Cu^{2+}; H_2CA = chloranilic acid ($C_6H_2O_4Cl_2$)) and uncoordinated guest molecules [13,60]. The chains which are linked by hydrogen bonds between the coordinated water and the oxygen atoms of the CA^{2-} anion on the adjacent chain form layers. The neutral guest molecules are intercalated between the $\{[M(CA)(H_2O)_2]_m\}_n$ layers, which are supported by $N\cdots H_2O$ hydrogen-bonding. Moreover, we also synthesized the 2-D hydrogen bond-supported sheets of the Fe–CA complex which intercalate ferrocenium cations [54]. The guest ferrocenium cations are intercalated in between the sheet by electrostatic and stacking interaction. The background of these researches prompted us to develop the coordination chemistry of the metal–chloranilate system. In this study, we have developed the new architecture of higher dimensional crystalline iron–chloranilate assemblies using different guest molecules. In this respect, we synthesized novel hydrogen bond-supported layered compounds, $\{(Hpy)[Fe(CA)_2(H_2O)_2](H_2O)\}_n$ (**1**) and $\{(H_2bipy)[Fe(CA)_2(H_2O)_2]_2(H_2O)_2\}_n$ (**2**). In both the structures, two CA^{2-} and two water molecules are coordinated to an iron ion and make the anionic building blocks $[Fe(CA)_2(H_2O)_2]^-$, which form the 2-D layers supported by hydrogen bonds. Guest molecules, Hpy^+ in **1** and H_2bipy^{2+} in **2** are included in between the layers. The synthesized compounds show varieties in the formation of layer structures, and in the inclusion mode. In this report we describe the crystal structures, thermal and magnetic properties of the two compounds.

2. Experimental

2.1. Syntheses

2.1.1. $\{(Hpy)[Fe(CA)_2(H_2O)_2](H_2O)\}_n$ (1)

An aqueous solution (1 ml) of iron(III) nitrate enneahydrate (3×10^{-6} mol) was transferred to a glass tube, then an ethanol–H_2O (1:5) solution (1 ml) of chloranilic acid (6×10^{-6} mol) and ethanol–H_2O (1:2) solution (1 ml) of pyridine (6×10^{-6} mol) were poured into the tube without mixing the three solutions. Black crystals began to form at ambient temperature in 1 week.

2.1.2. $\{(H_2bipy)[Fe(CA)_2(H_2O)_2]_2(H_2O)_2\}_n$ (2)

An ethanol–H_2O (1:9) solution (1 ml) of chloranilic acid (6×10^{-6} mol) was transferred to a glass tube, then an ethanol–H_2O (3:17) solution (1 ml) of iron(III) nitrate enneahydrate (4×10^{-6} mol) and ethanol–H_2O (1:4) solution (1 ml) of 4,4′-bipyridine (4×10^{-6} mol) were poured into the tube without mixing the three solutions. Dark-violet crystals began to form at ambient temperature in 1 week.

2.2. Physical measurements

The ^{57}Fe Mössbauer spectra were obtained using a Wissel Mössbauer spectrometer with a proportional counter. A ^{57}Co(Rh) source moving in a constant acceleration mode was used for the measurements. The velocity scale was calibrated by using a metallic iron-foil spectrum. The isomer shift (IS) and the quadruple splitting (QS) were obtained by least-squares fitting of the Mössbauer data to Lorentzian line shapes. Magnetic susceptibility data were recorded over the temperature range 2–300 K at 1 T with a SQUID susceptometer (Quantum Design, San Diego, CA). All data were corrected for diamagnetism, which were calculated from Pascal's table. Thermal gravimetric (TG) and differential scanning calorimetric (DSC) analysis were carried out with a Seiko Instruments SSC5200 thermoanalyzer in a nitrogen atmosphere (heating rate: 10 K min^{-1} for TG and 2–5 K min^{-1} for DSC).

2.3. Crystallographic data collection and refinement of the structure

A suitable crystal was chosen and mounted on glass fibers with epoxy resin. Data collections of compounds **1** and **2** were carried out on Rigaku AFC7R and Mac Science MXC3 automatic diffractometers, respectively. The structures were solved by direct methods (Rigaku texsan crystallographic software package of Molecular Structure Corporation). Full-matrix least-squares refinements were carried out with anisotropic thermal parameters for all non-hydrogen atoms. The final cycle of full-matrix least-squares refinement was based on *No* and *n* variable parameters and converged with unweighted agreement factors of $R = \Sigma\big||F_o| - |F_c|\big|/\Sigma|F_o|$, $Rw = [\Sigma(|F_o| - |F_c|)^2/\Sigma w|F_o|^2]^{1/2}$ where $w = 1/\sigma^2(F_o) = [\sigma_c^2(F_o) + p^2/4F_o^2]^{-1}$. Crystal data for **1**. $FeC_{17}O_{11}Cl_4NH_{12}$, Mw = 603.94, triclinic, space group $P\bar{1}$ (# 2), with $a = 9.537(5)$, $b = 13.563(6)$, $c = 9.231(4)$ Å, $\alpha = 107.18(4)$, $\beta = 102.33(4)$, $\gamma = 102.12(4)°$, $V = 1065.9(10)$ Å^3, $Z = 2$, $T = 23°C$, μ (Mo–K$_\alpha$) = 12.71 cm^{-1}, λ (Mo–K$_\alpha$) = 0.71069 Å, $n = 307$; *N*, *No* ($I > 3\sigma(I)$) = 5189, 4895; *R*, *Rw* = 0.068; 0.141, *p*-factor = 0.1930, goodness-of-fit indicator = 1.37. Crystal data for **2**. $Fe_2Cl_8C_{34}N_2O_{22}H_{22}$, Mw = 1205.87, triclinic, space group $P\bar{1}$ (# 2), with $a = 9.101(1)$, $b = 10.379(1)$, $c = 12.802(2)$ Å, $\alpha = 79.45(1)$, $\beta = 82.67(1)$, $\gamma = 66.32(1)°$, $V = 1086.8$ (3) Å^3, $Z = 1$, $T = 23°C$, μ (Mo–K$_\alpha$) = 12.46 cm^{-1}, λ (Mo–K$_\alpha$) = 0.71073 Å, $n = 340$; *N*, *No* ($I > 3\sigma(I)$) = 5431, 4995; *R*, *Rw* = 0.039; 0.036, *p*-factor = 0.0100, goodness-of-fit indicator = 1.62.

3. Results and discussion

3.1. Crystal structure *1*

An ORTEP drawing of the structure around the iron ion in **1** with the atom numbering scheme is shown in Fig. 1. The structure of **1** consists of mononuclear $[Fe(CA)_2(H_2O)_2]^-$ anions, Hpy^+ cations and uncoordinated water molecules. $[Fe(CA)_2(H_2O)_2]^-$ monomer is the building block of the host layer, which is formed by the coordination of two CA^{2-} and two water molecules in the *trans* position. The geometry around the iron ion in the building block is a distorted octahedron, which is similar to that of the building block in $\{[Fe(Cp)_2][Fe(CA)_2(H_2O)_2]\}_n$ (Cp^- = cyclopentadienyl anion) [54]. The distortion of octahedral geometry in **1** is observed from the Fe–O bond lengths. The $[Fe(CA)_2(H_2O)_2]^-$ anions in **1** form 2-D layers, spreading out along the *bc* plane. The layers are supported by four types of hydrogen bonds, which occur between the coordinated water molecules and the terminal oxygen atoms of CA^{2-} anion of adjacent building blocks, 2.662(7), O(5)–O(7); 2.695(8), O(5)–O(8), 2.714(7), O(6)–O(9); 2.721(7) Å, O(6)–O(10). The chlorine atoms of CA^{2-} project forward to the outside of the layer to create channels diagonally between the *b* and *c* axes. The uncoordinated Hpy^+ make hydrogen bonds with the interstitial water molecules (2.71(1) Å; O(11)–N), and are included in the channels by electrostatic interaction with the anionic host layer. Thus the electrostatic interaction between the host layer and the guest molecules plays an important role to construct the inclusion system and to expand its dimensionality. In the compound **1** the sandwiched molecules are included discretely in between the layers. Interestingly in addition to electrostatic interaction, Hpy^+ cations with interstitial water molecules are anchored alternatively to the layer by making two types of hydrogen bonds with the coordinated oxygens of CA^{2-}, 2.871(8); O(3)–O(11) and 2.950(9) Å; O(2)–O(11).

3.2. Crystal structure *2*

An ORTEP drawing of the structure around the iron ion in **2** with the atom numbering scheme is shown in Fig. 2. The structure of $\{(H_2bipy)[Fe(CA)_2(H_2O)_2]_2(H_2O)_2\}_n$ (**2**) consists of mononuclear $[Fe(CA)_2(H_2O)_2]^-$ anions, H_2bipy^{2+} cations and uncoordinated water molecules. Two CA^{2-} dianions and two water molecules are coordinated to the iron ion making the $[Fe(CA)_2(H_2O)_2]^-$ monomer, which is the building block of the host layer. The geometry around the iron ion in the building block is a distorted octahedron, similar to that of **1** but the two water molecules in **2** are coordinated to iron ion in the *cis* position relative to each other. The coordinated chloranilate rings of the building blocks are stacked upon each other with a nearest-neighbor C(3)–C(5′) distance of 3.339(4) Å and make a helical chain spreading diagonally between *b* and *c* axes. The chains are supported by two types of hydrogen bonds which occur

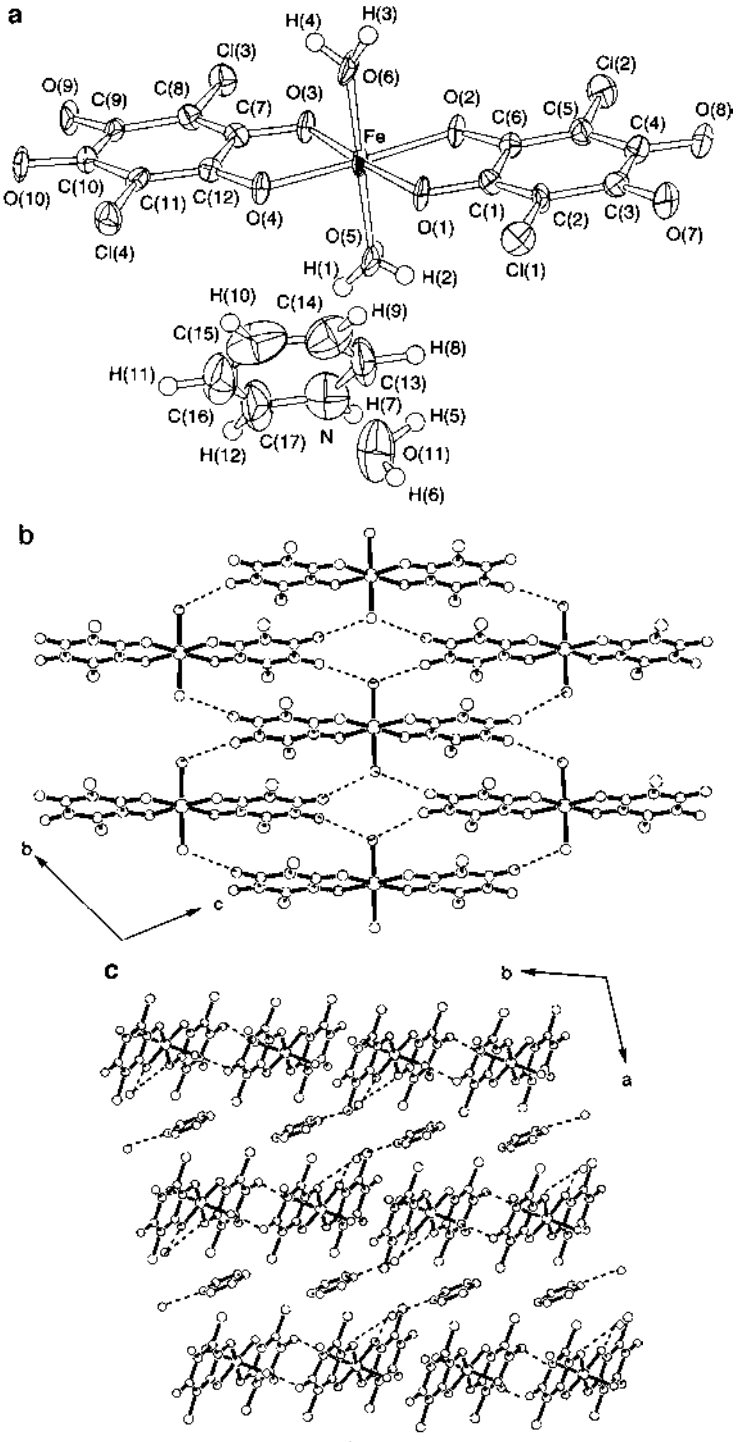
a
H(4)
H(3)
Cl(3)
O(6)
Cl(2)
O(9)
C(9)
C(8)
C(7)
O(3)
O(2)
C(6)
C(5)
C(4)
O(8)
Fe
O(10)
C(10)
C(11)
C(12)
O(4)
O(1)
C(1)
C(2)
C(3)
O(7)
Cl(4)
O(5)
H(1)
H(2)
Cl(1)
H(10)
C(14)
H(9)
C(15)
H(8)
H(11)
C(13)
H(7)
H(5)
C(16)
C(17)
N
H(12)
O(11)
H(6)
b
b
c
c
b
a

Fig. 1.

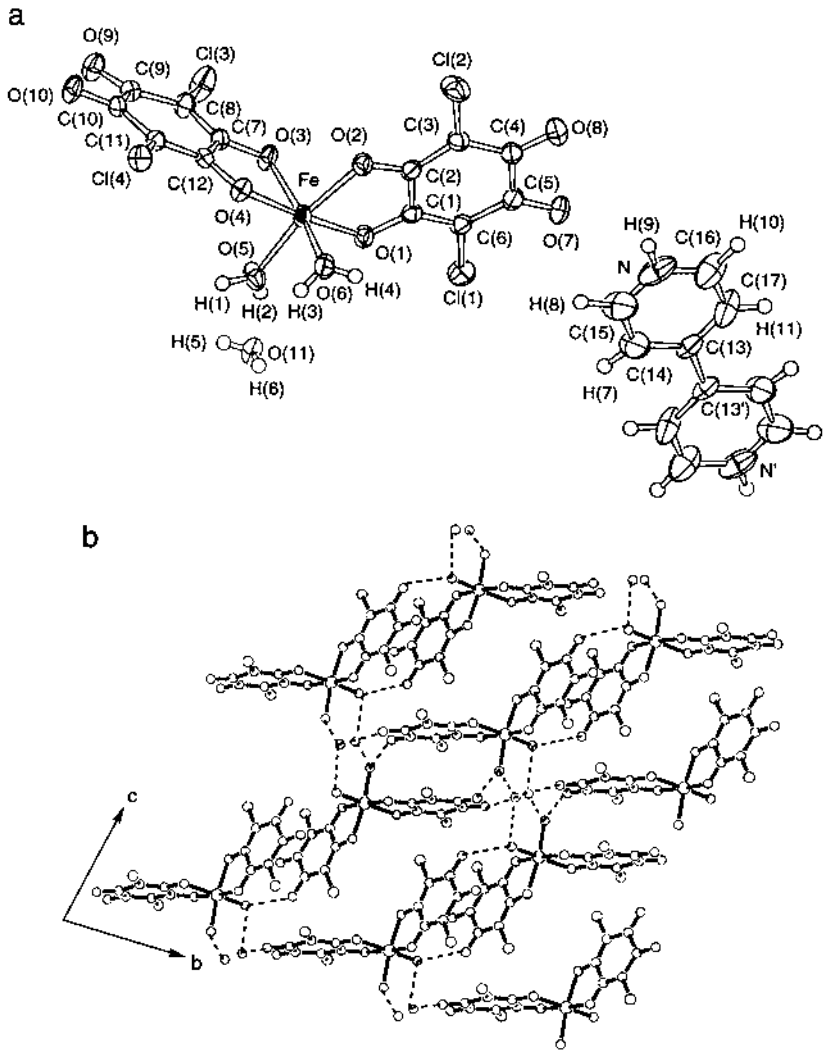

Fig. 2. (a) ORTEP drawing of a monomer unit of compound **2** with labeling scheme and thermal ellipsoids at the 50% probability level for Fe, Cl, O, N, and C atoms. Spheres of the hydrogen atoms have been arbitrarily reduced. Selected bond distances (Å) and angles (°); Fe–O(1), 1.975(2); Fe–O(2), 2.005(2); Fe–O(3), 2.010(2); Fe–O(4), 1.992(2); Fe–O(5), 2.007(3); Fe–O(6), 2.065(3); O(1)–Fe–O(2), 80.53(9); O(2)–Fe–O(3), 92.38(10); O(3)–Fe–O(4), 80.16(9); O(5)–O(10), 2.683(3); O(5)–O(11), 2.666(4); O(6)–O(8), 2.757(4); O(6)–O(11), 2.701(4); O(7)–N, 2.833(4); O(6)–O(11′), 2.746(4); O(6)–O(11), 2.945(3); O(10)–O(11), 2.807(3). (b) Layer of $[Fe(CA)_2(H_2O_2)]^-$; viewed onto *bc*-plane. (c) Assembled structure of **2**.

Fig. 1. (a) ORTEP drawing of a monomer unit of compound **1** with labeling scheme and thermal ellipsoids at the 50% probability level for Fe, Cl, O, N, and C atoms. Spheres of the hydrogen atoms have been arbitrarily reduced. Selected bond distances (Å) and angles (°); Fe–O(1), 1.961(5); Fe–O(2), 2.021(5); Fe–O(3), 1.991(4); Fe–O(4), 1.982(5); Fe–O(5), 2.044(6); Fe–O(6), 2.041(5); O(1)–C(1), 1.284(7); O(2)–C(6), 1.273(8); O(3)–C(7), 1.285(7); O(4)–C(12), 1.285(7); O(1)–Fe–O(2), 81.5(2); O(1)–Fe–O(3), 174.5(2); O(1)–Fe–O(4), 104.2(2); O(1)–Fe–O(5), 90.5(2); O(3)–Fe–O(4), 81.3(2); O(2)–O(11), 2.950(9); O(3)–O(11), 2.871(8); O(5)–O(7), 2.662(7); O(5)–O(8), 2.695(8); O(6)–O(9), 2.714(7); O(6)–O(10), 2.721; O(11)–N, 2.71(1). (b) Layer of $[Fe(CA)_2(H_2O)_2]^-$; viewed onto *bc*-plane. (c) Assembled structure of **1**.

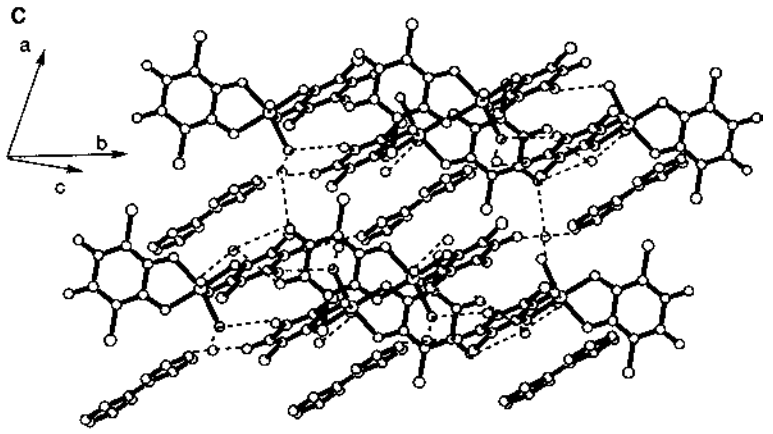

Fig. 2. (*Continued*)

between the coordinated water molecules and the terminal oxygens of CA^{2-}, 2.683(3); O(5)–O(10) and 2.757(4) Å; O(6)–O(8). The dihedral angle between the planes of two coordinated CA^{2-} in **2** is 104.0°. The coordination of water molecules in the *cis* position allows the building blocks to connect to each other in a helical fashion, supported by hydrogen bonding and stacking interaction. The chains make a 2-D layer spreading along the *bc* plane. The position of the interstitial water molecules is different in the two compounds, in **1** they are included into the layers with Hpy^{+} ions and in **2** they take part in the formation of the layers by connecting the chains supported by hydrogen bonds. In the layer of **2**, uncoordinated water molecules make four types of hydrogen bonds with coordinated water molecules and terminal oxygens of CA^{2-}, 2.666(4); O(5)–O(11), 2.701(4); O(6)–O(11), 2.945(3); O(9)–O(11), 2.807(3) Å; O(10)–O(11). The H_2bipy^{2+} cations are included in between the layers by electrostatic interaction with anionic host layers and by hydrogen bonding that occurs between the terminal oxygen atoms of CA^{2-} and protonated nitrogens of bipyridine rings, 2.833(4) Å; N–O(7). Moreover, the H_2bipy^{2+} ions are stacked with the planes parallel to the rings of coordinated CA^{2-} with a nearest-neighbor C(1)–C(17′) distance of 3.440(5) Å. The coplanarity of the bipyridine rings are observed in few compounds. In {[Co(NCS)$_2$(H$_2$O)$_2$(4,4′-bipy)](4,4′-bipy)}, the two pyridine rings are coplanar in both the coordinated and hydrogen bonded types of 4,4′-bipy ligands but no stacking between pyridine rings is observed [17]. In [Cd(4,4′-bipy)$_2$](NO$_3$)$_2$·2C$_6$H$_4$Br$_2$, coplanarity of coordinated bipy arises due to the interaction of solvent molecules, $C_6H_4Br_2$ with the host lattice [37]. There is no significant solvent interaction in the compound **2**, only a stacking interaction of the bipyridine rings with the planes of CA^{2-} anions makes the two rings to divert from the sterically more favorable non-coplanar arrangement to coplanar.

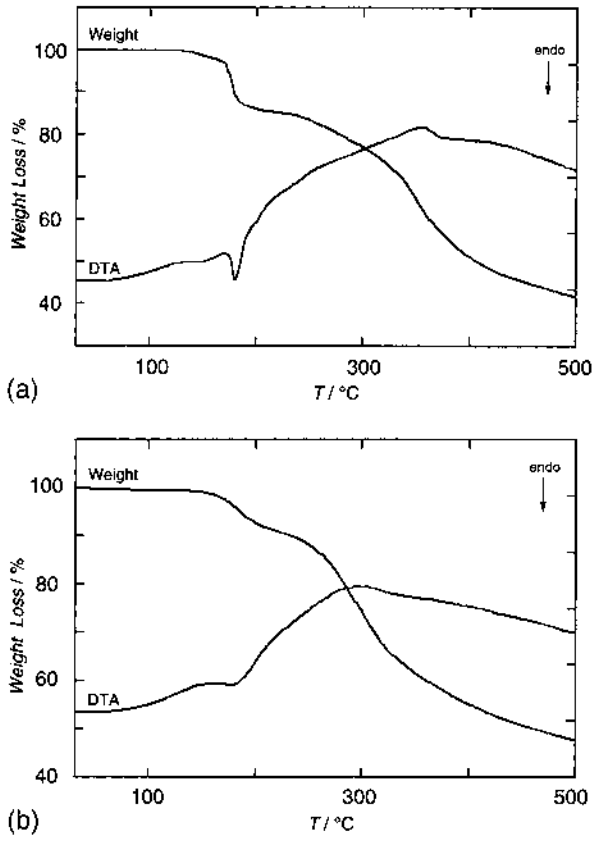

Fig. 3. Thermogravimetric analyses data for **1** (a) and **2** (b).

*3.3. Thermal properties of **1** and **2***

To observe the thermal stability and the host–guest interaction in **1** and **2**, TG and DSC measurements have been carried out under a nitrogen atmosphere. The TG diagram of **1** shows rapid changes at 150 and 180°C (Fig. 3(a)). The liberation of interstitial and coordinated water molecules account for the 3 and 10% weight losses at the above temperature ranges, respectively, indicating the easy release of the interstitial water molecules. The TG diagram of **2** shows weight loss at 185°C, which is higher than that of **1** (Fig. 3(b)). The weight change in **2** accounts for the liberation of water molecules, but in this case, we cannot distinguish between the interstitial and coordinated water molecules, because the interstitial molecules are strongly hydrogen-bonded with the CA^{2-} of the host layer and H_2bipy^{2+} ions. On the other hand, DSC traces of **1** show thermal anomaly at 174 K, indicative of a phase transition in the compound (Fig. 4), whereas **2** shows no DSC peak [61].

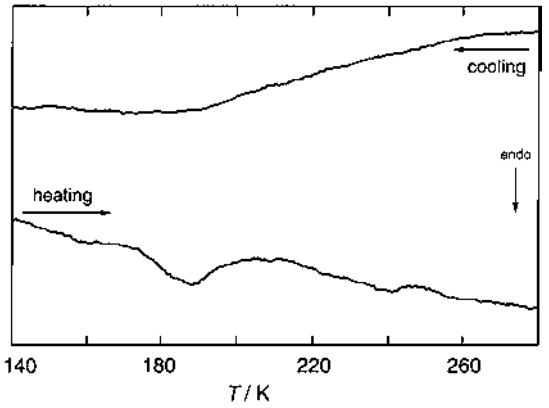

Fig. 4. DSC traces of **1**.

These thermal behaviors correlate well with the inclusion forces of the guest molecules in the compounds. In **1**, the Hpy^+ ions along with the interstitial water molecules can move in the channels, but in **2**, in addition to the hydrogen bonding and electrostatic interactions, H_2bipy^{2+} cations are stacked with the CA^{2-} planes.

3.4. Magnetic properties

The ^{57}Fe Mössbauer spectra of **1** and **2** consist of a single doublet with IS = 0.41 (**1**) and 0.39 mm s^{-1} (**2**); $QS = 0.83$ (**1**) and 1.29 mm s^{-1} (**2**) at 296 K, respectively. These values indicate that the oxidation state of iron in both the compounds is 3 with high-spin configuration ($S = 5/2$). The magnetic susceptibility (χ) of **2** was

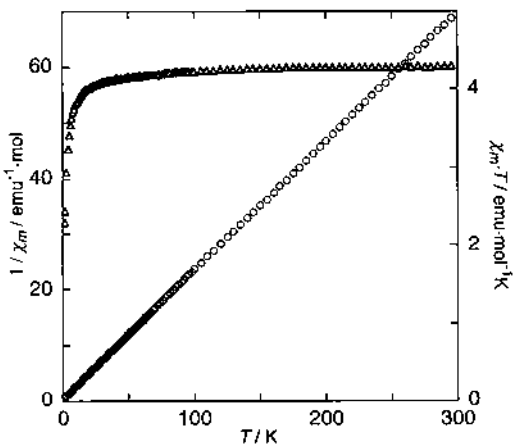

Fig. 5. Plots of observed $1/\chi_m$ and $\chi_m T$ vs. T for **2**.

measured over temperatures of 2–300 K (Fig. 5). The value of $\chi_m T = 4.30$ emu K mol^{-1} at 300 K also indicates the high-spin state of Fe(III) with $S = 5/2$. The $\chi_m T$ decreases slightly with decreasing temperature and at the lower temperature it decreases rapidly, indicative of the existence of a weak antiferromagnetic interaction ($\theta = -2.3$ K). This may be due to the spreading of magnetic ordering over the crystal. In this stage, we cannot determine the direction of the effective pathway of the exchange interaction, however, the value of θ is comparable to that of the coordination-bonded chain of $[Fe(CA)(H_2O)_2]_n$ in $\{(G)[Fe(CA)(H_2O)_2]\}_n$, suggesting that the spin–exchange interaction through hydrogen bonds in compound **2** is relatively higher than other hydrogen-bonded crystal structures [62,63].

4. Conclusions

In this study, we have constructed two new iron chloranilate complex assemblies, which contain the hydrogen-bonding linkage of the building blocks in the host assemblies and included guest molecules. Different guest molecules change the shape of the building blocks, which provide variety in the formation of the layer and in the inclusion mode. This proves that the formation of the building block is an important step to construct a metal–complex assembly. Hydrogen bonding interaction and electrostatic interaction are common driving forces for the inclusion of the guest molecules in the synthesized compounds. In addition, stacking interaction also plays an important role in the layer formation and inclusion of guest molecules. The hydrogen-bond supported host layer $\{[M(CA)_2(H_2O)_2]_k\}_1$ is so flexible that it allows one to include different sizes of guest molecules by changing the mode of assembly. Moreover the hydrogen-bonding interaction increases the dimensionality of the system and thus provides structural varieties in the crystal structures of iron–chloranilate assemblies.

Acknowledgements

This research was supported by a Grant-in-Aid for Scientific Research on Priority Areas (No. 10149101 'Metal-assembled Complexes') from the Ministry of Education, Science, Sports and Culture, Japan.

References

[1] G. De Munno, R. Ruiz, F. Lloret, J. Faus, R. Sessoli, M. Julve, Inorg. Chem. 34 (1995) 408.
[2] Y. Nagaoka, Phys. Rev. 147 (1966) 392.
[3] P. Delhaes, in: M. Drillon (Ed.), Organic and Inorganic Low Dimensional Crystalline Materials, Reidel, Dordrecht, 1987.
[4] D. Gatteschi, O. Kahn, J.S. Miller, F. Palacio (Eds.), Magnetic Molecular Materials, Reidel, Dordrecht, 1991, p. 198.
[5] D.W. Bruce, in: D. O'Hare (Ed.), Inorganic Materials, Wiley, New York, 1992.

[6] J.J. Borrás-Almenar, E. Coronado, C.J. Gómez-Garcia, L. Ouahab, Angew. Chem. Int. Ed. Engl. 32 (1993) 561.
[7] G. De Munno, M. Julve, F. Nicoló, F. Lloret, J. Faus, R. Ruiz, E. Sinn, Angew. Chem. Int. Ed. Engl. 32 (1993) 613.
[8] G. De Munno, D. Viterbo, A. Caneschi, F. Lloret, M. Julve, Inorg. Chem. 33 (1994) 1585.
[9] M. Julve, G. De Munno, G. Bruno, M. Verdaguer, Inorg. Chem. 27 (1988) 3160.
[10] T. Otieno, J.S. Rettig, R.C. Thompson, J. Trotter, Inorg. Chem. 32 (1993) 1607.
[11] Z.N. Chen, D.G. Fu, K.B. Yu, W.X. Tang, J. Chem. Soc. Dalton Trans. (1994) 1917.
[12] Z.N. Chen, J. Qiu, Z.K. Wu, D.G. Fu, K.B. Yu, W.X. Tang, J. Chem. Soc. Dalton Trans. (1994) 1923.
[13] S. Kawata, S. Kitagawa, H. Kumagai, C. Kudo, H. Kamesaki, T. Ishiyama, R. Suzuki, M. Kondo, M. Katada, Inorg. Chem. 35 (1996) 4449.
[14] H.J. Choi, M.P. Suh, J. Am. Chem. Soc. 120 (1998) 10 622.
[15] (a) T. Bein, Supramolecular Architecture: Synthetic Control in Thin Films and Solid, ACS Symposium Series 499, American Chemical Society, Washington, DC, 1992 (Ch. 19). (b) D.B. Amabilino, J.F. Stoddart, Chem. Rev. 95 (1995) 2725. (c) G.M. Whitesides, Sci. Am. (1995) 114. (d) J.-M. Lehn, Supramolecular Chemistry: Concepts and perspectives, VCH, Weinheim, 1995. (e) D.S. Lawrence, T. Jiang, M. Levett, Chem. Rev. 95 (1995) 2229 (f) T. Iwamoto, in: J.L. Atwood, J.E.D. Davies, D.D. MacNicol (Eds.), Inclusion Compounds, vol. 5, Academic Press, London, 1991, pp. 177–212.
[16] P. Bhyrappa, S.R. Wilson, K.S. Suslick, J. Am. Chem. Soc. 119 (1997) 8492.
[17] J. Lu, T. Paliwala, S.C. Lim, C. Yu, T. Niu, A.J. Jacobson, Inorg. Chem. 36 (1997) 923.
[18] W.T.S. Huck, R. Hulst, P. Timmerman, F.C. Veggel, D.N. Reinhoudt, Angew. Chem. Int. Ed. Engl. 36 (1997) 1006.
[19] M. Fujita, M. Aoyagi, F. Ibukuro, K. Ogura, K.J. Yamaguchi, J. Am. Chem. Soc. 120 (1998) 611.
[20] P.J. Stang, N.E. Persky, J. Manna, J. Am. Chem. Soc. 119 (1997) 4777.
[21] G.B. Gardner, D. Venkataraman, J.S. Moore, S. Lee, Nature 374 (1995) 792.
[22] J.D. Hartgerink, J.R. Granja, R.A. Milligan, M.R. Ghadiri, J. Am. Chem. Soc. 118 (1996) 43.
[23] P.R. Ashton, A.N. Collins, M.C.T. Fyfe, S. Menzer, J.F. Stoddart, D.J. Williams, Angew. Chem. Int. Ed. Engl. 36 (1997) 735.
[24] C. Janiak, Angew. Chem. Int. Ed. Engl. 36 (1997) 1431.
[25] J.A. Real, E. Andrés, M.C. Muñoz, M. Julve, T. Granier, A. Bousseksou, F. Varret, Science 268 (1995) 265.
[26] H.O. Stumpf, L. Ouhab, Y. Pei, D. Grandjean, O. Kahn, Science 261 (1993) 447.
[27] M. Fujita, J.K. Yoon, O. Sasaki, K. Yamaguchi, K. Ogura, J. Am. Chem. Soc. 117 (1995) 7287.
[28] J.A. Whiteford, C.V. Lu, P.J. Stang, J. Am. Chem. Soc. 119 (1997) 2524.
[29] S.R. Batten, B.F. Hoskins, R. Robson, J. Am. Chem. Soc. (1995) 5385.
[30] O.M. Yaghi, H. Li, T.L. Groy, J. Am. Chem. Soc. 118 (1996) 9096.
[31] S. Subramanian, M.J. Zaworotoko, Angew. Chem. Int. Ed. Engl. 34 (1995) 2127.
[32] T.L. Hennigart, D.C. Macquarrie, P. Losier, R.D. Rogers, M.J. Zaworotoko, Angew. Chem. Int. Ed. Engl. 36 (1997) 972.
[33] O.M. Yaghi, in: T.L. Pinnavania, M.F. Thrope (Eds.), Access in Nanoporous Materials, Plenum, New York, 1995, p. 111.
[34] S. Kawata, S. Kitagawa, H. Kumagai, S. Iwabuchi, M. Katada, Inorg. Chim. Acta 267 (1998) 143.
[35] G.S. Hanan, C.R. Arana, J.-M. Lehn, D. Fenske, Angew. Chem. Int. Ed. Engl. 34 (1995) 1122.
[36] M. Fujita, J. Yazaki, K. Ogura, J. Am. Chem. Soc. 112 (1990) 5645.
[37] M. Fujita, Y.J. Kwon, S. Washizu, K. Ogura, J. Am. Chem. Soc. 116 (1994) 1151.
[38] S. Subaramanian, S. Zaworoko, Angew. Chem. Int. Ed. Engl. 34 (1995) 89.
[39] L. Carlucci, G. Ciani, D.M. Proserpio, A. Sironi, Angew. Chem. Int. Ed. Engl. 34 (1995) 1895.
[40] G.M. Whiteside, E.E. Simanek, J.P. Mathias, C.T. Seto, D.N. Chin, M. Mammen, D.M. Gordon, Acc. Chem. Res. 28 (1995) 37.
[41] S.R. Breeze, S. Wang, Inorg. Chem. 32 (1993) 5981.
[42] C. Robl, W. Kuhs, J. Solid State Chem. 75 (1988) 15.
[43] C. Robl, S. Hentschel, G. McIntyre, J. Solid State Chem. 96 (1992) 318.

[44] S. Kawata, S. Kitagawa, H. Machida, T. Nakamoto, M. Kondo, M. Katada, K. Kikuchi, I. Ikemoto, Inorg. Chim. Acta 229 (1994) 211.
[45] T. Mitani, Mol. Cryst. Liq. Cryst. 171 (1989) 343.
[46] T. Inabe, K. Okinawa, H. Okamoto, T. Mitani, Y. Murayama, S. Takeda, Mol. Cryst. Liq. Cryst. 216 (1992) 229.
[47] K. Nakasuji, K. Sugiura, T. Kitagawa, J. Toyoda, H. Okamoto, K. Okinawa, T. Mitani, H. Yamamoto, I. Murata, A. Kawamoto, J. Tanaka, J. Am. Chem. Soc. 113 (1991) 1862.
[48] Q.C. yang, M.F. Richardson, D.J. Dunitz, J. Am. Chem. Soc. 107 (1985) 5535.
[49] M.T. Reetz, S. Hööger, K. Harm, Angew. Chem. Int. Ed. Engl. 33 (1994) 181.
[50] T. Zeegers-Huyskens, P.L. Huyskens, in: P.L. Huyskens, A.P. Luck, T. Zeegers-Huyskens (Eds.), Intermoleculer forces — An Introducion to Modern Methods and Results, 1991.
[51] C.B. Aakeröy, K.R. Seddon, Chem. Soc. Rev. (1993) 397.
[52] J.C. MacDonald, G.M. Whitesides, Chem. Rev. 94 (1994) 2383.
[53] H. Bock, W. Seitz, Z. Havlas, J.W. Bates, Angew. Chem. Int. Ed. Engl. 32 (1993) 411.
[54] S. Kawata, H. Kumagai, S. Kitagawa, K. Honda, M. Enomoto, M. Katada, Mol. Cryst. Liq. Cryst. 286 (1996) 51.
[55] M. Verdaguer, A. Michalowicz, N. Alberding, J.J. Girerd, O. Kahn, Inorg. Chem. 19 (1980) 3271.
[56] J.T. Wrobleski, D.B. Brown, Inorg. Chem. 18 (1979) 2738.
[57] S. Kawata, S. Kitagawa, M. Kondo, I. Furuchi, M. Munakata, Angew. Chem. Int. Ed. Engl. 33 (1994) 1759.
[58] S. Kawata, S. Kitagawa, M. Kondo, M. Katada, Synth. Met. 71 (1995) 1917.
[59] S. Kawata, S. Kitagawa, I. Furuchi, C. Kudo, H. Kamesaki, M. Kondo, M. Katada, M. Munakata, Mol. Cryst. Liq. Cryst. 274 (1995) 179.
[60] S. Kawata, S. Kitagawa, H. Kumagai, T. Ishiyama, K. Honda, H. Tobita, K. Adachi, M. Katada, Chem. Mater. 10 (1998) 3902.
[61] M.K. Kabir, S. Kawata, K. Adachi, H. Tobita, N. Miyazaki, H. Kumagai, M. Katada, S. Kitagawa, Mol. Cryst. Liq. Cryst. (1999) in press.
[62] S. Kawata, S.R. Breeze, S. Wang, J.E. Greedan, N.P. Raju, Chem. Commun. (1997) 717.
[63] L. Ballester, A. Gutiérrez, M.F. Perpiñán, U. Amador, M.T. Azcondo, A.E. Sánchez, C. Bellitto, Inorg. Chem. 36 (1997) 6390.
[64] J.V. Folgado, R. Ibáñez, E. Coronado, D. Beltrán, J.M. Savariault, J. Galy, Inorg. Chem. 27 (1988) 19.
[65] S. Decurtins, H.W. Schmalle, L. Zheng, J. Ensling, Inorg. Chim. Acta 244 (1996) 165.
[66] L. Zheng, H.W. Schmalle, S. Ferlay, S. Decurtins, Acta Crystallogr. Sect. C 54 (1998) 1578.